CHIN. PHYS. LETT. Vol. 36, No. 5 (2019) 057101

Temperature-Dependent Characteristics of GaN Schottky Barrier Diodes with TiN and Ni Anodes *

Ting-Ting Wang(王婷婷)[1], Xiao Wang(王霄)[1**], Xiao-Bo Li(李小波)[2],
Jin-Cheng Zhang(张进成)[1], Jin-Ping Ao(敖金平)[1,2**]

[1]*Key Laboratory of Wide Band-Gap Semiconductor Materials and Devices, School of Microelectronics, Xidian University, Xi'an 710071*
[2]*Institute of Technology and Science, Tokushima University, Tokushima 770-8506, Japan*

(Received 21 January 2019)

The effect of temperature on the characteristics of gallium nitride (GaN) Schottky barrier diodes (SBDs) with TiN and Ni anodes is evaluated. With increasing the temperature from 25 to 175°C, reduction of the turn-on voltage and increase of the leakage current are observed for both GaN SBDs with TiN and Ni anodes. The performance after thermal treatment shows much better stability for SBDs with TiN anode, while those with Ni anode change due to more interface states. It is found that the leakage currents of the GaN SBDs with TiN anode are in accord with the thermionic emission model whereas those of the GaN SBDs with Ni anode are much higher than the model. The Silvaco TCAD simulation results show that phonon-assisted tunneling caused by interface states may lead to the instability of electrical properties after thermal treatment, which dominates the leakage currents for GaN SBDs with Ni anode. Compared with GaN SBDs with Ni anode, GaN SBDs with TiN anode are beneficial to the application in microwave power rectification fields due to lower turn-on voltage and better thermal stability.

PACS: 71.55.Eq, 85.30.Hi, 73.20.−r, 73.43.Jn DOI: 10.1088/0256-307X/36/5/057101

Wireless microwave power transmission has been applied in electric vehicle battery charging, energy harvesting and wireless power distribution within buildings.[1] There are rf-to-dc conversion circuits, so-called rectenna, which is the key unit in the receiving terminal of a wireless power transmission system. The conversion efficiency of the receiving terminals depends strongly on the performance of the Schottky barrier diode (SBD) used in the rectification circuit, which includes the on-resistance, off-capacitance and turn-on voltage. To improve the conversion efficiency, reduction of ratio of the turn-on voltage to the breakdown voltage is important.[2] Gallium nitride (GaN) is an attractive material for SBDs due to its high-breakdown voltage, high-frequency operation and high-temperature performance.[3]

Recently, different anode materials such as Ni, W and Mo are applied in GaN SBDs. In our previous study, GaN SBDs with reactively sputtered TiN anode present a lower turn-on voltage compared with Ni anode, meanwhile the on-resistance, reverse leakage currents and reverse breakdown characteristics are comparable. Circuit simulation estimates that the conversion efficiency of the rectenna circuit with TiN anode SBDs will increase from 84% to 89% with the turn-on voltage decreasing from 1.0 to 0.5 V at 2.45 GHz.[4]

It is well known that the Schottky barrier characteristics vary with temperatures.[5–8] Moreover, the SBDs for rectenna will be used at various temperatures, mainly at elevated temperatures due to self-heating effects in high power rectification. In this study, the electrical characteristics of TiN anode SBDs are evaluated by experimental measurements and simulations at different temperatures, and the mechanisms of reverse leakage current are analyzed, together with Ni anode SBDs for comparison. The main leakage mechanisms are thermionic emission (TE) and phonon-assisted tunneling (PhAT). The TE process is that the electrons go across the metal-semiconductor barrier under the applied electric field, and the PhAT process is that the electrons tunnel from interface states to the semiconductor conduction band when the influence of interface states on the current-voltage characteristics is non-negligible.

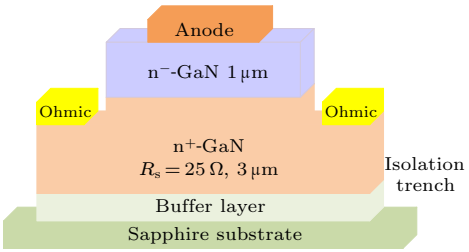

Fig. 1. The cross-sectional view of the GaN SBD.

Figure 1 shows the cross-sectional view of the GaN SBD. The epi-wafer is grown on a *c*-plane sapphire substrate with a buffer layer, an n^+-GaN access layer with an impurity density of over $4\times10^{18}\,cm^{-3}$ and an n^--GaN drift layer from the bottom to the top. The thickness of the access layer is about 3 μm with a sheet resistance of 25 Ω/square. The thickness of the drift layer is 1 μm with an impurity density of $1\times10^{17}\,cm^{-3}$, which is designed to achieve the reverse breakdown voltage over 100 V.

The fabrication process started from the drift layer mesa formation by etching down to the access layer

*Supported by the National Key Research and Development Plan under Grant No 2017YFB0403000, and the Fundamental Research Funds for the Central Universities under Grant No JB181110.
**Corresponding author. Email: x.wang@xidian.edu.cn; jpao@xidian.edu.cn
© 2019 Chinese Physical Society and IOP Publishing Ltd

with an inductively coupled plasma (ICP) dry etching system. Next, deep trench isolation down to the sapphire surface was formed using the same ICP system. After that, Ti/Al/Ti/Au (50/200/40/40 nm) was deposited by sputtering for cathode ohmic electrodes followed by an annealing at 850℃ for 1 min in N_2 ambient. Then, TiN/Ni/Au (10/5/5 nm) was deposited as the anode Schottky electrode. A TiN thin film was synthesized by reactive sputtering (dc, 75 W) in Ar:N_2 (15:3 sccm) mixed gas atmosphere under the chamber pressure of 0.14 Pa, using a metal target of Ti with a purity of 99.99%.[9,10] Samples with Ni/Au (10/10 nm) anode were also prepared for comparison by sputtering in Ar (30 sccm) atmosphere at 0.14 Pa and 10 W. Next, a Au film was electroplated with a thickness of about 1 μm all over the electrodes. Finally, post-annealing was performed at 300℃ for 10 min.

To investigate the temperature characteristics of the GaN SBDs, the current-voltage (I–V) characteristics of circular-type SBDs with radius of 50 μm were measured at the temperatures of 25, 75, 125, and 175℃, respectively. To monitor the degradation during the high temperature measurements, diodes were cooled down to room temperature before the measurements of high temperature I–V characteristics.

Figure 2 shows the forward I–V characteristics of the circular SBDs with TiN and Ni anodes (r = 50 μm). The turn-on voltages, which are defined as the voltage with the current density at 1 mA/mm, are 0.25 and 0.70 V for the TiN- and Ni-anode diodes at 25℃, respectively. The turn-on voltage decreases as the temperature increases, namely, 0.20, 0.15 and 0.10 V for the TiN SBD and 0.65, 0.55 and 0.45 V for the Ni SBD, at 75, 125 and 175℃, respectively.

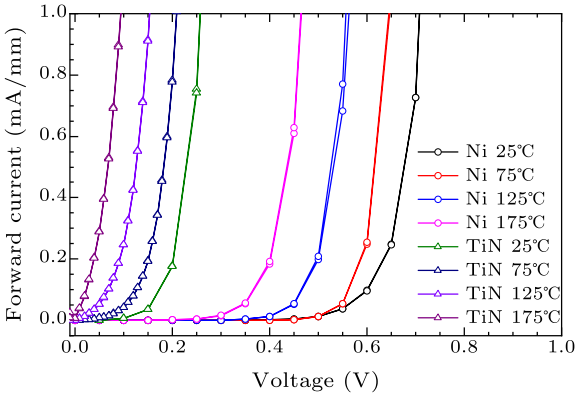

Fig. 2. Forward I–V characteristics of the diodes with TiN and Ni anodes in linear scales. The label TiN 25℃ is signified as the forward I–V characteristic of TiN anode SBD at 25℃. The label Ni 25℃ is signified as the forward I–V characteristic of Ni anode SBD at 25℃. The others are similar to this.

The measured I–V characteristics are analyzed using the thermionic emission theory for Schottky contacts. When $qV \geqslant 3kT$, the equation can be simplified to[11]

$$I = A_e A^* T^2 \exp\left(\frac{-q\phi_B}{kT}\right) \exp\left(\frac{qV}{nkT}\right), \qquad (1)$$

where A_e is the effective diode area, A^* is the effective Richardson constant, which is 24.0 $Acm^{-2}K^{-2}$ for n-type GaN, T is the absolute temperature, ϕ_B is the barrier height, V is the forward-bias voltage, k is the Boltzmann constant, and n is the ideality factor. Equation (1) can be converted into

$$\ln I = \frac{qV}{nkT} + \ln(A_e A^* T^2) - \frac{q\phi_B}{kT}. \qquad (2)$$

With this equation, ϕ_B and n can be determined from the intercept point and the slope of forward-bias I–V characteristic.

Figure 3 shows the Schottky barrier height and the ideality factor versus temperatures for the SBDs with TiN and Ni anodes. The barrier height and the ideality factor of the TiN SBD at room temperature are around 0.60 eV and 1.08. In contrast, they are around 1.01 eV and 1.10 respectively for the Ni SBD. The lower work function of TiN SBD is in accord with the lower turn-on voltage. For both the devices, it is found that the barrier height increases and the ideality factor decreases with the increasing temperature. The increase of the barrier height is attributed to the effect of barrier inhomogeneity.[12–14] That is, as temperature increases, higher energy carriers are enhanced and the average barrier height for thermionic emission will increase. As shown in Fig. 3, the barrier height of TiN SBD varies slightly, while that of Ni SBD varies more, indicating that the interface characteristic of TiN SBD is much more stable than that of Ni SBD, due to fewer defect in TiN/GaN Schottky contact. The ideality factors converge to unity at higher temperature for both the devices because the thermionic emission dominates at higher temperatures compared with other mechanisms.

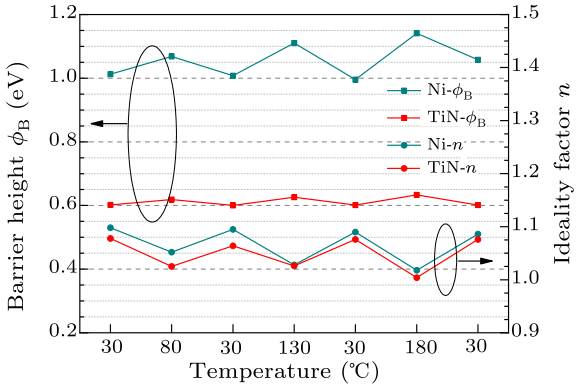

Fig. 3. The Schottky barrier height and ideality factor under different temperatures for the SBDs with TiN and Ni anodes.

From the logarithmic plots of current-voltage characteristics, as shown in Fig. 4(a), all the room temperature curves of the TiN SBD after high temperature treatment almost remain unchanged compared to the original room temperature curve, while these of the Ni SBD indicate an obvious discrepancy after high temperature treatment, as shown in Fig. 4(b). Both of TiN and Ni SBDs have almost the same order of reverse leakage current magnitude at room temperature. After the temperature-bias stress, the current-voltage curves of Ni SBD cannot return to the initial current-voltage curve when back to room temperature. In ad-

dition, the interface charges of TiN SBD are less than those of Ni SBD at 25℃ according to the dual voltage sweep curves. Thus the TiN SBD shows a better thermal stability than the Ni SBD.

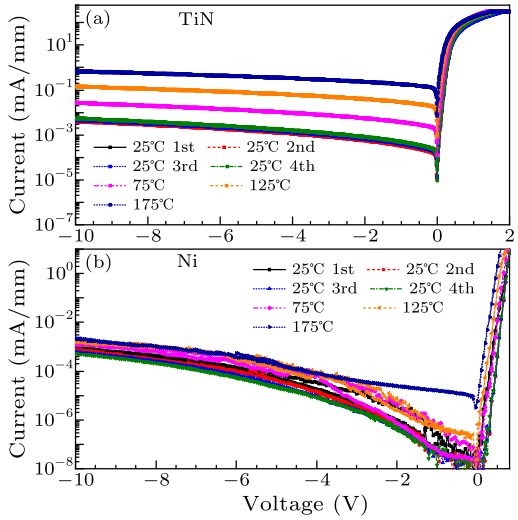

Fig. 4. The I–V characteristics of (a) TiN and (b) Ni SBDs under different temperatures. The labels 25℃ 1st, 75℃, 125℃ and 175℃ are signified as the I–V characteristic of TiN or Ni anode SBD at 25℃, 75℃, 125℃ and 175℃, respectively, and the labels 25℃ 2nd, 25℃ 3rd, and 25℃ 4th are signified as the I–V characteristic of TiN or Ni anode SBD when back to 25℃ after high temperature treatment at 75, 125 and 175℃, respectively.

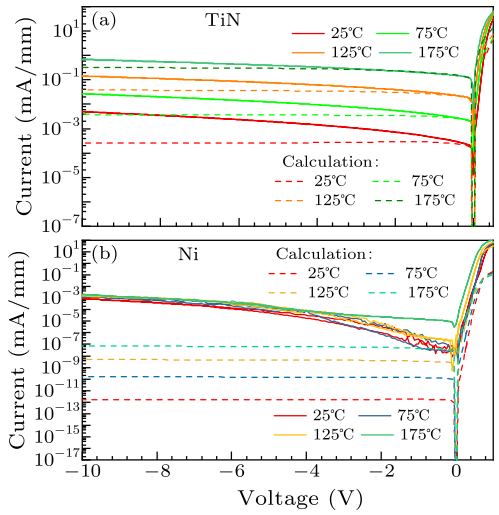

Fig. 5. The comparison between the experimental current-voltage characteristics for (a) TiN and (b) Ni SBDs simulated by the TE model. The labels such as 25℃ and 25℃ calculation are respectively signified as the experimental data and the simulated I–V characteristics of TiN- or Ni-anode SBDs at 25℃.

To study the leakage mechanisms of TiN and Ni SBDs, the TE model is firstly applied to calculate the leakage currents. Figure 5 shows the comparison between the experimental and the simulated reverse leakage currents of the TiN and Ni SBDs, respectively. The simulated current is calculated using the TE model by Silvaco TCAD setting the work functions of 4.7 and 5.15 eV for TiN and Ni SBDs, respectively.[4] The calculated leakage currents for the TiN SBD in Fig. 5(a) agree well with the experimental results at low bias level, indicating that thermionic emission mechanism dominates the reverse leakage current of the TiN SBD. The increase of the leakage current at higher bias is attributed to the image-force lowering, which is ignored in the calculation. Moreover, the simulated leakage currents for the Ni SBD as shown in Fig. 5(b) are much lower than the experimental data, indicating that the other mechanisms except the TE model may dominate the reverse leakage current of Ni SBDs. Interface charges between Ni metal and the GaN material may form amounts of interface states leading to the PhAT effect.[15–17]

The reason for different reverse leakage current characteristic of two diodes is the metal work function and interface charge differences. Hence, the simulations of temperature-dependent characteristics of reverse leakage current have to analyze different metal work functions and different interface charges for TiN- and Ni-anode diodes. Therefore, two kinds of Schottky diode reverse leakage mechanisms, i.e., phonon-assisted electron tunneling and thermionic emission, are applied.[18–22]

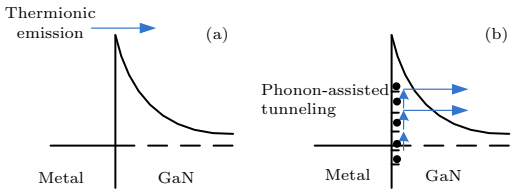

Fig. 6. (a) Thermionic emission model, and (b) phonon-assisted tunneling model.

As shown in Fig. 6(a), the thermionic emission process is that the electrons go across the metal-semiconductor barrier under the applied electric field. The thermionic emission current meets the formula (1). As shown in Fig. 6(b), phonon-assisted electron tunneling mechanism occurs when the influence of interface states on the current-voltage characteristics is non-negligible.[23,24] For the traps with Dirac wells, the PhAT current meets[8]

$$J = eN_{\rm s}W, \tag{3}$$

where e, $N_{\rm s}$ and W are respectively the electronic charge, the occupied state density near the interface, and the rate of phonon assisted tunneling of electrons from localized states into the conduction band. The rate of phonon-assisted tunneling W, as functions of temperature T and field strength E, is[8]

$$\begin{aligned} W = {} & \frac{eE}{8m^*\varepsilon_T}[(1+\gamma^2)^{1/2}-\gamma]^{1/2}[1+\gamma^2]^{-1/4} \\ & \times \exp\left\{\frac{-4}{3}\frac{(2m^*)^{1/2}}{eE\hbar}\varepsilon_T{}^{3/2}[(1+\gamma^2)^{1/2}-\gamma]^2\right. \\ & \left.\times\left[(1+\gamma^2)^{1/2}+\frac{\gamma}{2}\right]\right\}, \end{aligned} \tag{4}$$

where

$$\gamma = \frac{(2m^*)^{1/2}\Gamma^2}{8e\hbar E(\varepsilon_T)^{1/2}}, \tag{5}$$

and E, ε_T, m^* and $\hbar$ are respectively the field strength at the interface, the trap depth, the relative effective mass for electrons and the reduced Planck constant,

and Γ is the energy width of the absorption band given by[8]

$$\Gamma^2 = 8a(\hbar\omega)^2(2n_{\rm p}+1), \tag{6}$$

with $n_{\rm p}$, a and $\hbar\omega$ being the phonon density, the electron-phonon interaction constant and the phonon energy, respectively.[8]

Two kinds of current mechanism are applied in the simulation as the TE and the PhAT models. The TE model is strongly dependent on the temperature and metal-semiconductor contact barrier height. The PhAT model is mainly related to the interface states and the impurity levels.[8] The reverse leakage current of TiN and Ni SBDs is calculated by Silvaco TCAD and their sizes are set as the same. The temperature range is from 25℃ to 175℃. The simulated device structure and material parameters are designed as the same as in Fig. 1. The TE model is set the same as the above with the metal work function at 4.7 or 5.15 eV for TiN or Ni SBD, while in the PhAT model, the occupied state density near the interface is set at $1.5\times10^{15}/{\rm cm}^2$.

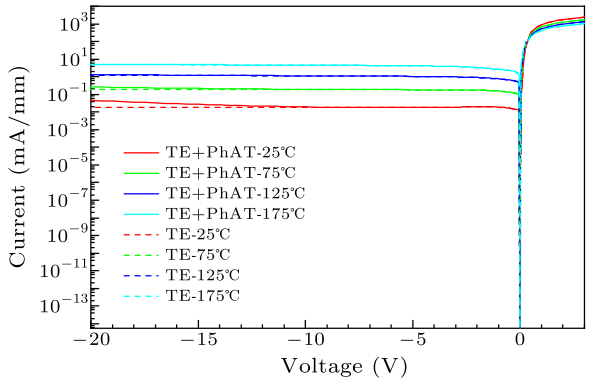

Fig. 7. The theoretical I–V characteristics of the TiN Schottky barrier diode simulated at 25–175℃ in steps of 50℃. The label TE+PhAT-25℃ means the combined result of both the TE and PhAT models at 25℃, and the label TE-25℃ means the result of only the TE model at 25℃.

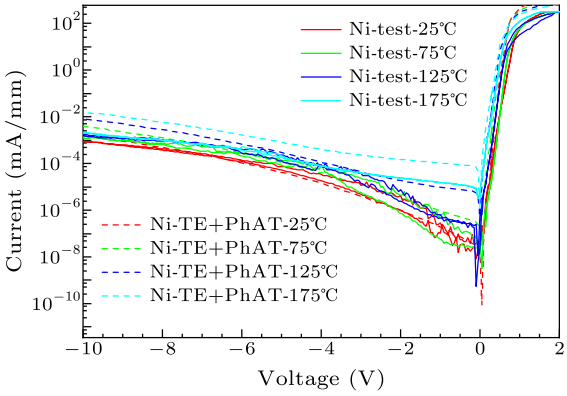

Fig. 8. The simulated I–V curves (dashed lines) by the TE and PhAT models and the experimental I–V curves (solid lines) of the Ni SBD from 25 to 175℃. The label Ni-TE+PhAT-25℃ means the combined result of both the TE model and the PhAT model at 25℃ for the Ni SBD. The label Ni-test-25℃ means the experimental results for the Ni SBD at 25℃.

In Fig. 7, the reverse leakage current of the TiN SBD is calculated by the TE model and the PhAT model. The simulation results (dashed lines) are calculated by the TE model and the simulation results (solid lines) are calculated by both the TE model and the PhAT model. Obviously, the thermionic emission current dominates in the TiN SBD at low bias level. In Fig. 8, the experimental I–V curves (solid lines) and the theoretical I–V curves simulated by the TE and PhAT models (dashed lines) of the Ni SBD are demonstrated from 25℃ to 175℃. The order of reverse leakage current magnitudes for the Ni SBD simulated only by the TE model ranges approximately from −7 to −12 at −10 V bias as shown in Fig. 5(b). In contrast, the order of reverse leakage current magnitudes calculated by the TE and PhAT models ranges approximately from −2 to −3 at −10 V bias as shown in Fig. 8, which is distinctly close to the experimental curves. Hence, the PhAT reverse leakage current plays a dominant role in Ni SBDs.

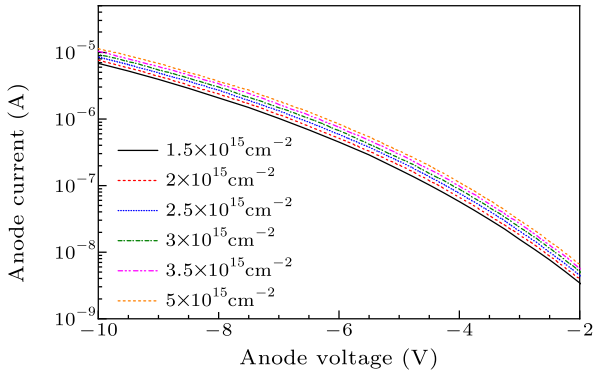

Fig. 9. The reverse leakage current with different occupied state densities for the Ni SBD at 25℃. The number 1.5×10^{15} cm^{-2} is the occupied state density.

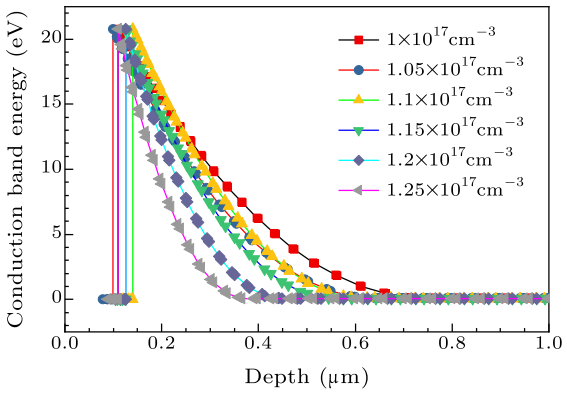

Fig. 10. The Schottky barrier width with different interface charge concentrations for the Ni SBD. The number 1×10^{17} cm^{-3} is the interface charge density.

As is known, the PhAT model is influenced by the interface states. To further confirm this, different occupied state densities are simulated. As shown in Fig. 9, the simulation results indicate that the reverse leakage current of Ni anode SBD increases obviously when the occupied state density increases slightly. It is speculated that Ni metal at the interface may be oxidized at high temperature and Ni–N–Ga bonds may be oxidized as Ni–O–Ga bonds so that the electron con-

centration at the Schottky interface increases, leading to the narrower barrier width as shown in Fig. 10 and the significant increased reverse leakage current.

In summary, we have investigated the temperature-dependent characteristics of TiN and Ni SBDs from 25 to 175℃. The turn-on voltage decreases and the Schottky barrier height increases for both the TiN and Ni SBDs with increasing temperature. Compared with the Ni SBD, lower turn-on voltage of 0.32 V for the TiN SBD is observed at 25℃, which can be ascribed to the lower Schottky barrier height of about 0.60 eV in TiN contact. In addition, reverse leakage current for the TiN SBD shows no degradation after high temperature measurements, while the reverse leakage current with serious degradation is observed in the Ni SBD, indicating better thermal stability in the TiN SBD. Furthermore, the reverse current-voltage characteristic for TiN SBDs agrees well with the simulated TE model, while that for the Ni SBDs is much higher than the results simulated only by the TE model. Further simulation results reveal that the main reverse leakage current mechanism of Ni SBDs is phonon-assisted tunneling and the reason for the reverse leakage current of Ni SBDs may be the interface charges possibly due to the oxidation of interface chemical bonds after thermal treatment. Lower turn-on voltage and better thermal stability lying in TiN SBDs are beneficial to the application in microwave power rectification fields.

References

[1] Hershtig R 2011 *IEEE Microwave Mag.* **12** 64
[2] Hayashino K, Harauchi K, Iwasaki Y, Fukui K, Ao J P and Ohno Y 2012 *Int. Microowave Workshop Ser. Innovative Wireless Power Transmission* (Kyoto Japan 10–11 May 2012) p 179
[3] Takahashi K, Ao J P, Ikawa Y, Hu C Y, Kawai H, Shinohara N, Niwa N and Ohno Y *J. Appl. Phys.* **48** 04C095
[4] Li L A, Kishi A, Liu Q, Itai Y, Fujihara R, Ohno Y and Ao J P 2014 *IEEE J. Electron Devices Soc.* **2** 168
[5] Sawada T, Ito Y, Kimura N, Imai K, Suzuki K and Sakai S 2002 *Appl. Surf. Sci.* **190** 326
[6] Osvald J, Kuzmik J, Konstantinidis G, Lobotka P and Georgakilas A 2005 *Microelectron. Eng.* **81** 181
[7] Yıldırım N, Ejderha K and Turut A 2010 *J. Appl. Phys.* **108** 114506
[8] Pipinys P and Lapeika V 2006 *J. Appl. Phys.* **99** 093709
[9] Ao J P, Naoi Y and Ohno Y 2013 *Vacuum* **87** 150
[10] Li L A, Kishi A, Shiraishi T, Jiang Y, Wang Q and Ao J P 2014 *J. Vac. Sci. Technol. A* **32** 02B116
[11] Sze S M 2007 *Physics of Semiconductor Devices* (New York: John Wiley &Sons) chap 3 p 156
[12] Mtangi W, van Rensburg P J J, Diale M, Auret F D, Nyamhere C, Nel J M and Chawanda A 2010 *Mater. Sci. Eng. B* **171** 1
[13] Zhou Y, Wang D, Ahyi C, Tin C C, Williams J and Park M 2007 *J. Appl. Phys.* **101** 024506
[14] Iucolano F, Roccaforte F, Giannazzo F and Raineri V 2007 *J. Appl. Phys.* **102** 113701
[15] Saadaoui S, Salem M, Gassoumi M, Maaref H and Gaquière C 2011 *J. Appl. Phys.* **110** 013701
[16] Kim H, Schuette M, Jung H, Song J, Lee J, Lu W and Mabon J C 2006 *Appl. Phys. Lett.* **89** 053516
[17] Kawanago T, Kakushima K, Kataoka Y, Nishiyama A, Sugii N, Wakabayashi H, Tsutsui K, Natori K and Iwai H 2014 *IEEE Trans. Electron Devices* **61** 785
[18] Pipinys P, Pipiniene A and Rimeika A 1999 *J. Appl. Phys.* **86** 6875
[19] Tian H W, Zhang X Y and Bu Y Y 2018 *ACS Sustainable Chem. Eng.* **6** 7346
[20] Zhang H, Miller E J and Yu E T 2006 *J. Appl. Phys.* **99** 023703
[21] Miller E J, Yu E T, Waltereit P and Speck J S 2004 *Appl. Phys. Lett.* **84** 535
[22] Turuvekere S, Karumuri N, Rahman A A, Bhattacharya A, DasGupta A and DasGupta N 2013 *IEEE Trans. Electron Devices* **60** 3157
[23] Shiojima K, Suemitsu T and Ogura M 2001 *Appl. Phys. Lett.* **78** 3636
[24] Kumar A, Vinayak S and Singh R 2011 *J. Nano-Electron. Phys.* **3** 671